Recent model submarine experiments with the MDTF

Mackay, M.; Williams, C. D.; Derradji-Aouat, A.

8th Canadian Marine Hydromechanics and Structures Conference [Proceedings], 2007

Recent Model Submarine Experiments with the MDTF

Mike Mackay[1], Christopher D. Williams[2], and Ahmed Derradji-Aouat[2]

[1] *Defense R&D Canada Atlantic, P.O. Box 1012, Dartmouth, NS, B2Y 3Z7, Canada*

[2] *NRC Institute for Ocean Technology, P.O. Box 12093, St. John's, NL, A1B 3T5, Canada*

Email: *mike.mackay@drdc-rddc.gc.ca*

Abstract

DRDC and NRC–IOT have collaborated on testing a model of the Victoria class submarines at IOT in St. John's. Hydrodynamic coefficients derived from these experiments will be used in numerical models to simulate manoeuverability and emergency recovery. We summarize the test programs and results so far, and illustrate derivation of the principal coefficients. A qualitative comparison is made with other data and semiempirical predictions. An additional test program scheduled for late 2007 will complete the experimental component of this work.

1. Introduction

Static and dynamic towing tank experiments have been done with the Albert model of the Canadian Victoria class submarines. It was tested on the Marine Dynamic Test Facility (MDTF) at the National Research Council Canada (NRC) Institute for Ocean Technology (IOT) in St. John's, NL; Albert is officially designated IOT model 590. The work was sponsored by Defence R&D Canada (DRDC) and is part of an ongoing collaboration between DRDC Atlantic and NRC–IOT. The experiments to date comprise a program of static yaw and pitch tests done in 2004 and dynamic sway and yaw tests done in 2006. Additional dynamic experiments will take place in 2007.

The principal objective for DRDC is to validate and improve current numerical models for predicting submarine manoeuverability. Reduction of data from the experiments included deriving hydrodynamic manoeuvering coefficients. DRDC uses a coefficient based code to calculate the Victoria class Manoeuvering Limitation Diagram, which combines simulations of recovery from sternplane jams and flooding to define a set of safe operating envelopes in speed-depth space as outlined in section 8. Since the MDTF is capable of higher incidences and rotational rates than previously used test facilities, numerical models based on experiments with it should better represent the extreme conditions encountered during emergency recovery. The experiments will also add to the knowledge base for the submarines and will aid in evaluating full scale trials data as part of fine tuning the simulation codes.

This paper presents an overview of the 2004 and 2006 experiments, and of the subsequent analysis and coefficient derivation. Because of the operational sensitivity of submarine performance, specific results discussed here have been sanitized for publication.

2. Model Experiments

The Albert model is designed to be mounted on a sting attached to the MDTF sketched in figure 1. The MDTF is a five degree of freedom captive test

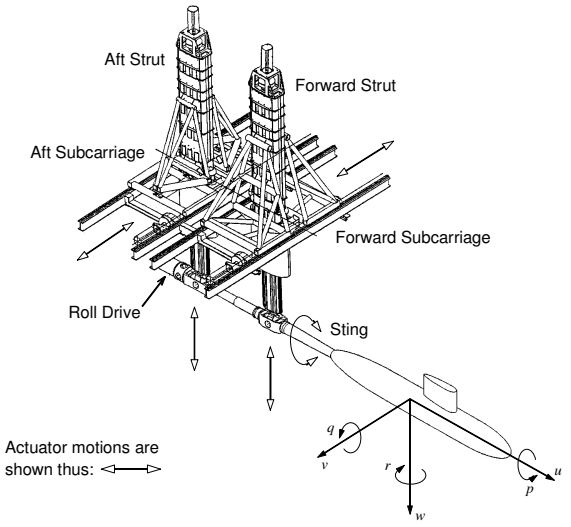

Figure 1. MDTF general arrangement.

rig which was jointly procured and funded by DRDC and NRC. It was built by Bombardier Inc. of Montreal and commissioned in October 1998. The MDTF can manoeuver a subsurface or surface captive model up to 6 metres long in any simultaneous combination of heave, pitch, sway and yaw motions through computer controlled electric servo actuators. When in use it is installed on the carriage of the IOT 200 m x 12 m x 7 m towing tank. The capability to use large models mitigates the problem of Reynolds scaling and has proven cost effective in allowing small underwater vehicles themselves to be tested without constructing a model. An account of MDTF development is given in reference [1], and its use and capabilities are discussed in reference [2].

The Albert model, figure 2, is nominally 1/15 scale, truncated at the tail to accommodate the sting, with a form displacement of about 930 kg in fresh water. Loads on the model are measured by an internal six component balance. Additional standard instrumentation on the model includes three orthogonal accelerometers forward and three aft, inclinometers for pitch and roll, and one or two inertial sensing systems each incorporating three accelerometers and three rate gyros.

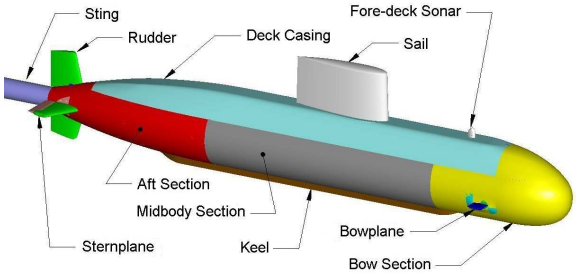

Figure 2. Albert model principal features.

The following discussions use standard notation (see reference [3] and the sketch at the end of this paper). X, Y, Z, K, M, N are the total loads on the model measured by the balance; they represent the axial, lateral, and normal forces, and roll, pitch, and yaw moment respectively. The corresponding translational velocities and angular rates are u, v, w, p, q, r. Euler angles about the axial, lateral, and normal axes are ϕ, θ, ψ. Submarine length is ℓ and LCG is x_G. Other quantities are defined in reference [3]. The coordinate origin for moment measurements and rotational motion is the balance resolution center, which is located on the hull axis at the nominal LCB of the full scale submarine.

Large loads are generated on the test rig and model during testing, and the structural compliance of the MDTF (and to a lesser extent of the balance and model) under load results in deviations in the model trajectory. At present the onboard instrumentation has to account for these. Additional external model tracking will be deployed in future experiments to better determine the deviations and develop appropriate correction methods.

The 2004 experimental program comprised static tests done with a number of model configurations. All the results discussed here are for the fully appended model including bowplanes. The 2006 program comprised primarily dynamic tests with the fully appended model, although some with other configurations, and some additional static tests, were planned. Unfortunately, the program was curtailed by electrical failure of vertical load cells in the balance. However, axial and lateral loads could be measured, so MDTF-generated motions were restricted to v and r. All the dynamic data discussed here are for simple harmonic motion.

3. Coefficient Regression

The coefficients in this paper are based on the Gertler and Hagen model of the standard submarine equations of motion [3] (hereafter G&H). Variants of it are the most commonly used coefficient models of submarine hydrodynamics. The basic G&H model applies to a fully submerged submarine at depth sufficient for the proximity of the surface to be ignored.

To extract coefficients, the equations of motion are recast in terms of the loads measured by the balance, retaining only those terms that are nonzero in the model experiment. There is insufficient room to present the full equations here; however, their general form is illustrated by the abbreviated expression for normal force:

$$\begin{aligned} Z \;=\; & \tfrac{1}{2}\rho\ell^4\left[\left(Z'_{\dot q} + m' x'_G\right)\dot q + Z'_{rr} r^2 + \ldots\right] + \\ & \tfrac{1}{2}\rho\ell^3\left[\left(Z'_{\dot w} - m'\right)\dot w + Z'_{vr} vr + \ldots\right] + \\ & \tfrac{1}{2}\rho\ell^2\left[Z'_{*} u^2 + Z'_{w} uw + \ldots\right] + \\ & (W - B)\cos\theta\cos\phi \end{aligned}$$

$Z'_*, Z'_w, \ldots, Z'_{\dot q}$, are the hydrodynamic coefficients. Primed quantities are nondimensionalized, i.e.,

$$m' = \frac{m}{\frac{1}{2}\rho\ell^3}\;,\quad x'_G = \frac{x_G}{\ell}\;,\quad Z'_* = \frac{Z_*}{\frac{1}{2}\rho\ell^2}\;,\quad \text{etc.}$$

We shall hereafter ignore hydrostatic terms such as $(W-B)\cos\theta\cos\phi$, in which W and B are the weight and buoyancy as seen by the balance load cells. These terms are eliminated from the data by tares or by measuring the inertial properties of the model.

There is a distinction between manoeuvering coefficients, which are the values derived from the full range of incidence or velocity, and stability derivatives, which are derived from near-zero incidence or velocity data only. The former are likely more accurate for simulating extreme manoeuvers, but stability derivatives may be used in a hybrid model as noted below. For small-perturbation stability analysis, the stability derivative is required.

To regress coefficients, static data were fitted with the Levenberg-Marquardt iterative least-squares algorithm implemented in Origin 7.5 software (OriginLab Corporation). Analysis of the dynamic data was a two step process. First, one of the motion parameters was fit with a sinusoid to establish amplitude, frequency, and phase. This gave nominal state variable time histories to which the load time histories were then fitted. The Levenberg-Marquardt algorithm was used to fit the data in both steps of the process.

4. Static Measurements

4.1 Pitch

Reducing the G&H equations for Z and M to static pitch terms, we obtain the following expressions:

$$\begin{aligned} Z &= \tfrac{1}{2}\rho\ell^2\left[Z'_* u^2 + Z'_w uw + Z'_{w|w|} w|w| + \right. \\ &\qquad \left. Z'_{|w|} u|w| + Z'_{ww} w^2\right] \\ M &= \tfrac{1}{2}\rho\ell^3\left[M'_* u^2 + M'_w uw + M'_{w|w|} w|w| + \right. \\ &\qquad \left. M'_{|w|} u|w| + M'_{ww} w^2\right] \end{aligned}$$

Analysis of the axial force, X, data was limited because of the presence of the sting [4,5]. X coefficients obtained in this study are included in the summary, section 7.

Data were acquired with the model upright and on its side: upright, the pitch angle is obtained more accurately by the on-board inclinometer. Regression on the equations above included 5 parameter fits, 3 parameter fits (i.e., omitting the last two minor terms), and linear regression of data within ± 2 or ± 5 degrees then substituting those values for a hybrid fit. In a hybrid fit, Z'_w and M'_w are stability derivatives. The difference in magnitudes of the principal coefficients in a 5 parameter hybrid fit relative to those from a regular fit was between 7 and 12 percent. However, this does not imply a comparable difference in the overall fit: in figure 3 the difference for Z is barely discernible, whereas for M it is evident but still small. Larger differences were found comparing 5 and 3 parameter fits. The relative goodness of each or any regression is to some extent subjective; some investigators prefer to use a hybrid fit in order to retain the stability derivatives.

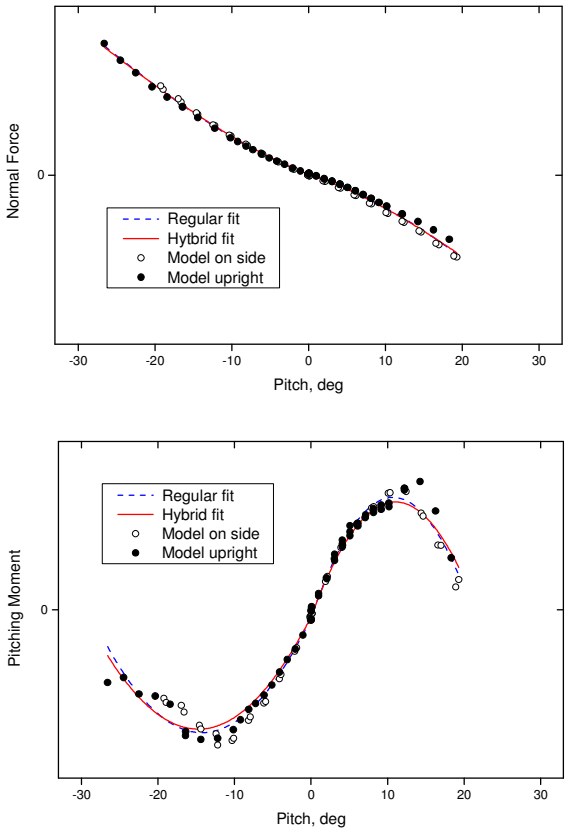

Figure 3. Normal force and pitching moment: comparison of regular and hybrid fits.

4.2 Yaw

Reducing the Y, K and N (in-plane load) equations to static yaw terms, we obtain:

$$\begin{aligned} Y &= \tfrac{1}{2}\rho\ell^2\left[Y'_v uv + Y'_{v|v|} v|v|\right] \\ K &= \tfrac{1}{2}\rho\ell^3\left[K'_v uv + K'_{v|v|} v|v|\right] \\ N &= \tfrac{1}{2}\rho\ell^3\left[N'_v uv + N'_{v|v|} v|v|\right] \end{aligned}$$

In yaw, the angle is obtained more accurately from runs with the model on its side than when it is upright. Nevertheless, the in-plane load data had little scatter even at large yaw angles, and regular and hybrid regression fits were quite similar.

In yaw there are also out-of-plane loads Z and M:

$$Z = \tfrac{1}{2}\rho\ell^2\left[Z'_* u^2 + Z'_{vv} v^2 + Z'_{vvvv}\frac{v^4}{U^2}\right]$$
$$M = \tfrac{1}{2}\rho\ell^3\left[M'_* u^2 + M'_{vv} v^2 + M'_{vvvv}\frac{v^4}{U^2}\right]$$

where we have added coefficients Z'_{vvvv} and M'_{vvvv} to model a reflex characteristic in the data. Comparison of regression fits with and without the additional coefficients is shown in figure 4. The extent to which this reflex, which is regularly observed in model tests [6], occurs at full scale has not yet been established.

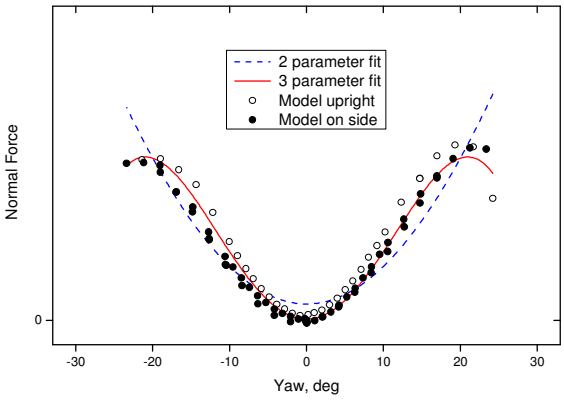

Figure 4. Out-of-plane normal force: comparison of 2 and 3 parameter fits.

4.3 Control Deflections

These are illustrated by the control loads due to a sternplane deflection δ_s:

$$Z = \tfrac{1}{2}\rho\ell^2\left[Z'_* + Z'_{\delta s}\delta_s\right]u^2$$
$$M = \tfrac{1}{2}\rho\ell^3\left[M'_* + M'_{\delta s}\delta_s\right]u^2$$

The G&H model has additional terms dependent on propulsion RPM that we have omitted.

Linear regression of the control loads generally gives a reasonable approximation of the data as shown for sternplane Z in figure 5. There may be a slightly higher slope in the data at small deflection angles, but it is not significant for manoeuvering simulations. An analogous trend, but with a lower inner slope, is generally observed when vehicle incidence is the variable [7].

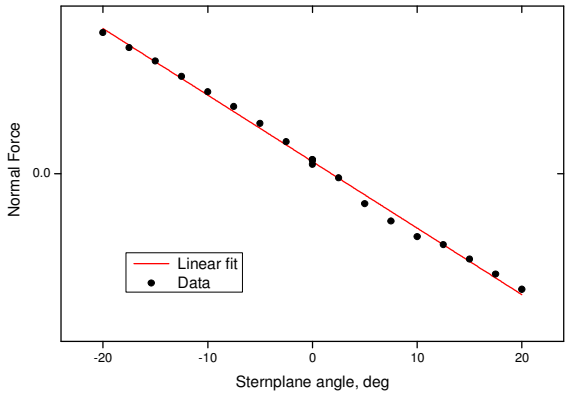

Figure 5. Sternplane normal force due to deflection.

5. Dynamic Measurements

5.1 Sway

The load cell problem prevented measurement of rolling moment. Reducing the Y and N equations to dynamic sway terms, we obtain:

$$Y = \tfrac{1}{2}\rho\ell^3\left(Y'_{\dot v} - m'\right)\dot v + \tfrac{1}{2}\rho\ell^2\left[Y'_v uv + Y'_{v|v|} v|v|\right]$$
$$N = \tfrac{1}{2}\rho\ell^4\left(N'_{\dot v} - m' x'_G\right)\dot v + \tfrac{1}{2}\rho\ell^3\left[N'_v uv + N'_{v|v|} v|v|\right]$$

To extract coefficients, the load data were referenced to the model lateral acceleration, which was fit with a sinusoid: $\dot v = A\sin(Bt + C)$. Since $\dot v$ is the measured acceleration, amplitude A incorporates model and rig deflections under load, but in other respects this is an idealized model of the motion. The maximum equivalent yaw observed in these experiments was about 5.7 degrees, essentially within the linear region with respect to yaw for the static tests, so the contribution of $v|v|$ terms to the loads was found to be negligible.

In conventional PMM terminology, e.g., in Booth [8], the coefficients Y'_v, $Y'_{\dot v}$, etc., obtained from experiments with small amplitude and low frequency are slow motion derivatives as opposed to oscillatory coefficients. Booth's simplified analysis defines slow motion derivatives as the limits of the oscillatory derivatives as frequency tends to zero, enabling them to be estimated by

extrapolation from harmonic test data. He attributes differences between the derivatives and coefficients to the omission of higher order terms and time history effects from the former. Coefficient models are conventionally assumed to be based on slow motion derivatives, and time history effects are seldom modeled. This is the case in the G&H equations; the later Feldman model [9] attempts to include them.

Dynamic experiments were done with varying amplitude and frequency. Of the sway coefficients, Y'_v was virtually independent of amplitude, figure 6, as required by Booth's analysis. The others showed irregular dependence on both amplitude and frequency, although their overall variation was less. Plotting Y'_v against the square of frequency f to estimate the slow motion derivative at $f = 0$ as the intercept of a linear regression, figure 7, yields a value that is 5 to 10 percent less than estimates from static yaw experiments.

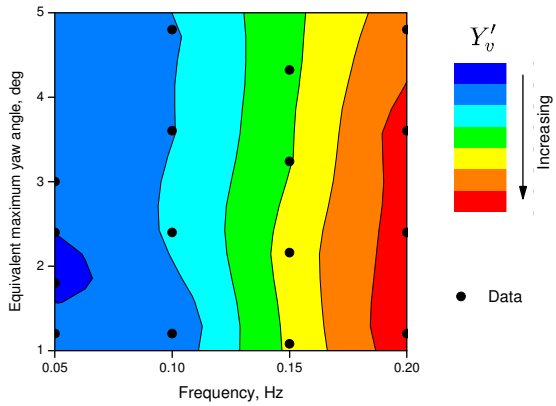

Figure 6. Dynamic sway Y'_v contours for frequency and amplitude dependence.

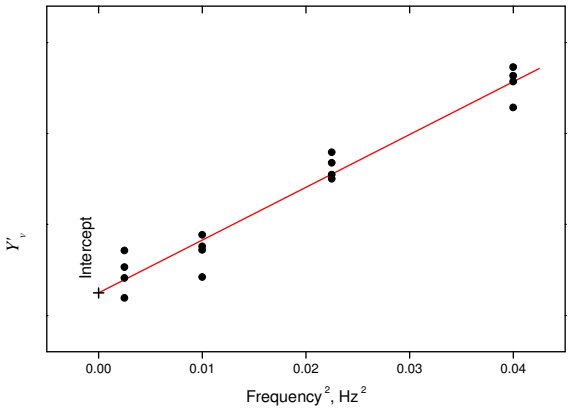

Figure 7. Dynamic sway linear regression of Y'_v against the square of frequency.

5.2 Yaw

Reducing the Y and N equations to dynamic yaw terms, we obtain:

$$\begin{aligned} Y &= \tfrac{1}{2}\rho\ell^4 \left(Y'_{\dot r} - m' x'_G\right)\dot r + \\ &\quad \tfrac{1}{2}\rho\ell^3 \left(Y'_r - m'\right) ur \\ N &= \tfrac{1}{2}\rho\ell^5 \left[\left(N'_{\dot r} - I'_z\right)\dot r + N'_{r|r|} r|r|\right] + \\ &\quad \tfrac{1}{2}\rho\ell^4 \left(N'_r - m' x'_G\right) ur \end{aligned}$$

We have assumed $y_G = 0$. The contribution of the term in $r|r|$ was found to be negligible. To extract coefficients, the load data were referenced to the measured yaw rate, which was fit with a sinusoid: $r = A\sin(Bt + C)$. The rate amplitude A therefore incorporates model and rig deflections under load.

Fitting the load data was complicated by high noise levels at the lowest frequencies. Dependence on amplitude and frequency was irregular for these coefficients, but again variability was low and we could not distinguish slow motion derivatives.

6. Experimental Uncertainty

The sources of systematic error in these experiments include model irregularities, instrumentation calibration error, and model and rig deflections under load. Analysis of stochastic errors leads to confidence intervals that are quite small. For example, as a percentage of the maximum load the 95% confidence intervals are at most about one percent. However, systematic errors are generally harder to identify and control, and are typically dominant. Thus while a large stochastic confidence interval indicates a large uncertainty in the estimated coefficient, a small interval does not imply small uncertainty.

Examination of noise in the load signals from both static and dynamic tests suggests the presence of a harmonic component that we attribute to balance vibrations. As we have made only a preliminary examination of the data and there are still a number of uncertainty issues to be resolved, formal analysis of all sources of error has been postponed until after the forthcoming 2007 test program.

Nevertheless, variation in the dynamic data is consistent with a few percent uncertainty in the derived coefficients, which is typical for towing tank and wind tunnel experiments. Accuracy of the static data results is expected to be similar, and comparable with that found in previous test pro-

grams. In an extensive comparison of MDTF experiments with the Standard Model [10] there was excellent agreement with results from a number of other facilities.

7. Coefficient Summary

Although not directly providing a measure of accuracy or uncertainty, it is instructive to compare coefficients derived from these tests with experimental values from UK experiments done during the design of the submarines, and with estimates from the geometry-based semiempirical code DSSP21 [7]. For this purpose, coefficient values with the lowest estimated uncertainty have been selected; some from hybrid regression fits, some not. In the comparative bar charts, figure 8, our experimental and DSSP21 results are referenced to the UK data, which represent a historical baseline. Differences in these charts do not indicate which value is correct for our purposes, but point to areas for further investigation. However, there is reasonable agreement between values for most of the principal coefficients.

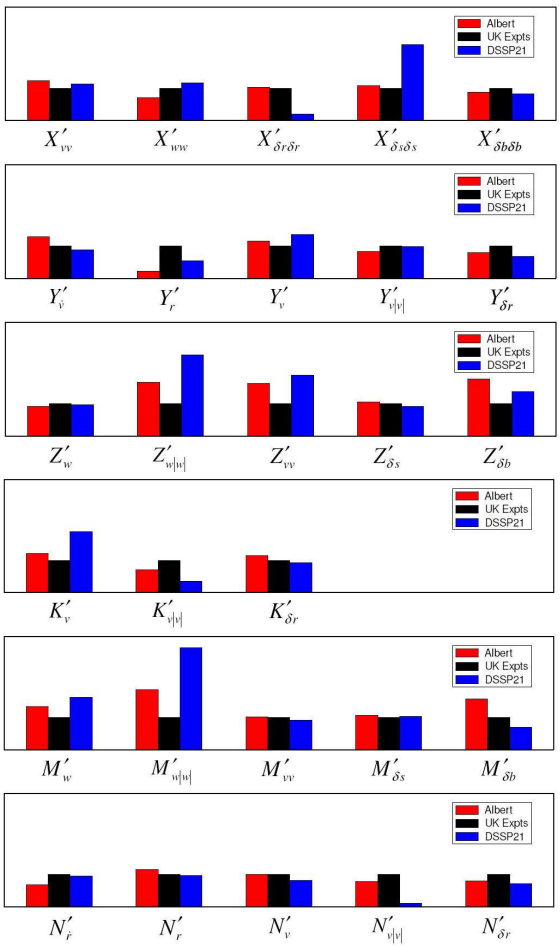

Figure 8. Coefficient estimates compared with UK and DSSP21 values.

8. Applications

DRDC Atlantic has used model experiments and numerical simulations based on them to study a number of performance and safety related issues for submarines, including the effect of towing an array, inadvertent loss of ballast, and the implications of adding a hull plug, or extension.

In the immediate future, Albert model test data will contribute to a review and possible revision of the current Manoeuvering Limitation Diagram (MLD). The MLD provides guidance to the operator; it defines sets of safe operating envelopes as illustrated in figure 9.

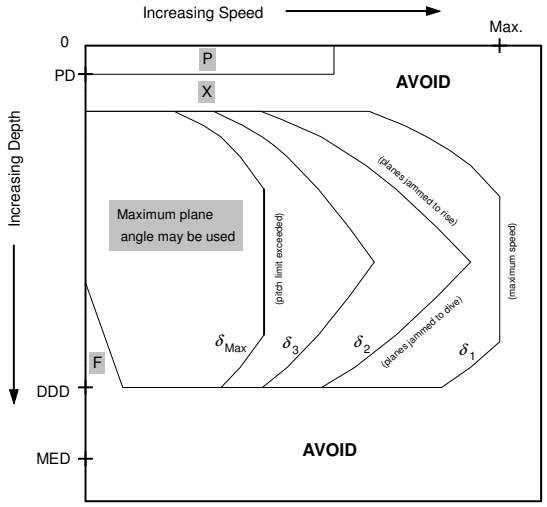

Figure 9. Schematic of a typical MLD; see text for legend.

On the figure, PD is periscope depth, DDD is deep diving depth, MED is maximum excursion depth, P is for passage to or from the surface only, X is to be avoided in shipping lanes, and F is the flood avoidance zone. A family of operating envelopes are shown for sternplane deflection limits $\delta_1 < \delta_2 < \delta_3 < \delta_{\text{Max}}$. The envelope boundaries are established by the success or failure of simulated emergency recoveries [11]. Lower boundaries are adjusted for shallow water operation. Generally more than one such diagram is required to define the operating limits of a particular submarine. Several thousand simulations are required to generate a complete MLD.

9. 2007 Experiments

The 2007 experimental program will complete, and selectively repeat, the 2006 program. In so doing, some issues have to be addressed. One is that circular arc data ($r \neq 0$, $\dot{r} = 0$) obtained in 2006 were not successfully analyzed because a combination of low turning rates and high acceleration in the transition between arcs resulted in signal-to-noise ratios that were too low; the arc manoeuvers will be redesigned. Another is the significance of frequency dependence in dynamic tests, which still has to be determined for many of the coefficients.

10. Concluding Remarks

We have outlined the 2004 and 2006 experimental programs with the Albert submarine model and discussed the derivation of coefficients for a numerical simulation model by means of classical regression methods. The results presented here are preliminary; corroboration and additional results will be obtained from experiments planned for late 2007.

The coefficients are derived from the Gertler and Hagen equations of motion [3]. These equations are adequate to validate and fine-tune the software presently used at DRDC Atlantic for MLD generation, but may need to be extended for future applications. For example, out-of-plane load measurements suggest that additional higher order terms are required in the equations. Other enhancements, including near-surface and near bottom influences for littoral manoeuvering, will require further experimentation following the 2007 program.

To complete the basic set of coefficients for the Albert model, parameters for the 2007 program will be chosen to alleviate some of the problems encountered in earlier tests, and other methods of analysis will be investigated if necessary. Comparison with coefficient predictions from DSSP21 is encouraging; aspects of this code may be incorporated into the simulation model.

Acknowledgements

We gratefully acknowledge the contributions of IOT and DRDC to this collaboration. We also thank the IOT staff — too numerous to mention individually — who were involved in the preparation and conduct of these experiments.

References

1. Fudge, G. and Mackay, M. (2003). Marine Dynamic Test Facility — a brief Development History. IOT LM–2003–01. National Research Council Canada Institute for Ocean Technology.

2. Williams, C.D., Mackay, M., Muselet, C., and Perron, C. (2002). Physical Modelling of Vehicle Performance in High-Amplitude and High-Rate Manoeuvres. In *Symposium on Challenges in Dynamics, System Identification, Control, and Handling Qualities for Land, Air, Sea, and Space Vehicles*. RTO–MP–095. NATO.

3. Gertler, M. and Hagen, G.R. (1967). Standard Equations of Motion for Submarine Simulation. NSRDC Report 2510. Naval Ship Research and Development Center.

4. Mackay, M. (1993). A Review of Sting Support Interference and some Related Issues for the Marine Dynamic Test Facility (MDTF). DREA Report 93/107. Defence Research Establishment Atlantic.

5. Beaver, W. (2007). Impact of Sting Mounting on Submarine Resistance. 28^{th} American Towing Tank Conference. University of Michigan, Ann Arbor.

6. Mackay, M. (2004). A Review of Submarine Out-of-Plane Normal Force and Pitching Moment. DRDC TM 2004–135. Defence R&D Canada – Atlantic.

7. Mackay, M. (2007). Semiempirical Component Based Modeling of Submarine Hydrodynamics and Systems: the DSSP21 (build 061102) Companion. DRDC TR 2007–039. Defence R&D Canada – Atlantic. (In printing.)

8. Booth, T.B. (1973). Oscillatory Testing of Ship Models. In *Journal of Sound and Vibration*, Vol. 28(4), pp 687–698.

9. Feldman, J. (1979). DTNSRDC Revised Standard Submarine Equations of Motion. DTNSRDC SPD–0393–09. David Taylor Naval Ship Research and Development Center.

10. Mackay, M. (2003). The Standard Submarine Model: A Survey of Static Hydrodynamic Experiments and Semiempirical Predictions. DRDC TR 2003–079. Defence R&D Canada – Atlantic.

11. Haynes, D., Bayliss, J., and Hardon, P. (2002). Use of the Submarine Research Model to Explore the Manoeuvring Envelope. In *Warship 2002: Naval Submarines 7*. London: Royal Institution of Naval Architects.

Coordinate System

The axial, lateral, and normal axes are x, y, and z respectively. $U^2 = u^2 + v^2 + w^2$. Other notation is given in section 2 of the text.